

Bridging the microscopic and macroscopic theories for light reflected from disordered plane-parallel dielectric slabs

S. Menon, Q. Su, and R. Grobe

Intense Laser Physics Theory Unit and Department of Physics, Illinois State University, Normal, Illinois 61790-4560 USA

(Received 14 February 2003; published 28 October 2003)

For a system of randomly arranged plane-parallel dielectric layers with randomly varying index of refraction and width, we compare the reflection coefficient derived from the Maxwell equations with that of the Boltzmann theory. For a strictly monochromatic field this coefficient is an oscillatory function of the laser frequency. We show how suitable frequency or ensemble averaging permits a comparison of the two theories. The calculation of the usual Boltzmann scattering coefficient from microscopic parameters can be improved to permit a better agreement with the exact Maxwell data.

DOI: 10.1103/PhysRevE.68.046614

PACS number(s): 42.25.Fx, 05.60.Cd, 73.50.-h

I. INTRODUCTION

The propagation of electromagnetic fields through highly scattering dielectric media is a subject of interest in many areas of science [1–3]. There is a wide variety of applications in meteorology, oceanography, medical imaging and therapy, astrophysics, radar transmission and reception, semiconductor technology, and photonic devices. The wave-medium interaction can be described by microscopic or macroscopic theories [4]. The precise relationship between these approaches, however, remains an open question [5].

The microscopic description is exact and requires a detailed knowledge of the medium, such as the location, the shape, and the index of refraction of each scatterer. Electromagnetic waves propagating through a microscopic medium of random scatterers can be analyzed rigorously using the Maxwell equations. These equations incorporate interference, diffraction, and polarization effects [5]. However, this approach is feasible numerically only for either reduced dimensional systems such as those with specific symmetries, or small systems that consist of a limited number of scatterers.

The macroscopic description is provided by the Boltzmann (radiative transport) equation. It is regarded in many areas of science as one of the most fundamental descriptions of the transport properties of particles in highly scattering or collisional media. In areas such as astrophysics and nuclear physics, the Boltzmann equation models the average motion of real particles such as neutrons [6,7]. In medical optics, the Boltzmann equation models the propagation of electromagnetic radiation through highly scattering biological materials [8–12].

There are certain length scales at which the Boltzmann theory is insufficient because some wave or diffraction effects are not negligible, but the system is too complicated to solve the corresponding Maxwell equations. It is this intermediate regime for which there is apparently no theoretical description available. A major research goal over the last few years has been to find an appropriate description for this mesoscopic regime. In this respect, it is important to notice that so far the Boltzmann equation can be derived only from phenomenological considerations, and its rigorous derivation even from the basic scalar wave Maxwell equation is not

available [4,5]. As a consequence, it is not clear how to relate the macroscopic scattering coefficient to the large number of microscopic variables, such as the spatially fluctuating index of refraction. Some progress has been reported in this regard in investigating the special case of stationary and homogeneous free fields in the absence of any turbid medium [13].

Therefore a better understanding of the relationship between the Boltzmann and Maxwell theories is important. Without too much loss of generality, this problem can be approached using a simple model system, for which the solutions to the Boltzmann and Maxwell equations are available. In such a one-dimensional system the light is restricted to scatter only in the forward and backward directions. In recent work we tried to connect the Boltzmann with the Maxwell description and found that the transmission coefficient for an ensemble average can be related to the predictions of the Boltzmann theory [14,15]. The present work is another step toward this long term goal.

In this work we will show that the Maxwell and Boltzmann equations for the one-dimensional system can be brought into a similar form. These equations have the advantage that perturbative but fully analytical solutions may be compared. We will show that an average of the Maxwell data over a suitable range of the laser frequency leads to a reflection coefficient that is similar to the one predicted by the Boltzmann equation.

II. FORMAL ANALOGY BETWEEN THE MAXWELL AND BOLTZMANN EQUATIONS

Let us first discuss how the time and spatial evolution of a laser field through a one-dimensional highly scattering medium can be described by the Maxwell as well as the Boltzmann theories. We will see that these seemingly different types of equations can be brought into a similar form if rewritten in terms of coupled equations relating the forward and backward propagating contributions of the fields.

We start the discussion with the Maxwell theory. The Maxwell equations for a position-dependent nonmagnetic dielectric medium [with permittivity $\epsilon(\mathbf{r})$ and permeability μ_0] are given by

$$\nabla \cdot \epsilon(\mathbf{r})\mathbf{E} = 0, \quad (2.1a)$$

$$\nabla \cdot \mathbf{B} = 0, \quad (2.1b)$$

$$\nabla \times \mathbf{E} = -\partial \mathbf{B} / \partial t, \quad (2.1c)$$

$$\nabla \times \mathbf{B} = \varepsilon(\mathbf{r}) \mu_0 \partial \mathbf{E} / \partial t. \quad (2.1d)$$

If the field is normally incident on a medium whose refractive index varies only along the x direction, these equations take the forms

$$\frac{\partial B_z(x,t)}{\partial t} = -\frac{\partial E_y(x,t)}{\partial x}, \quad (2.2a)$$

$$\varepsilon(x) \frac{\partial E_y(x,t)}{\partial t} = -\frac{1}{\mu_0} \frac{\partial B_z(x,t)}{\partial x}, \quad (2.2b)$$

$$\frac{\partial B_y(x,t)}{\partial t} = \frac{\partial E_z(x,t)}{\partial x}, \quad (2.2c)$$

$$\varepsilon(x) \frac{\partial E_z(x,t)}{\partial t} = \frac{1}{\mu_0} \frac{\partial B_y(x,t)}{\partial x}, \quad (2.2d)$$

where $E_{y,z}$ and $B_{y,z}$ are the transverse components of the electric and magnetic fields. Full solutions can be obtained only numerically, using either time-dependent methods for initial value problems [16] or other techniques for boundary value problems [17].

The model medium whose optical propagation properties we will examine in this work consists of a series of N lossless dielectric slabs arranged along the positive x axis, each of which is centered at position x_j , has a width w_j , and an index of refraction n_j ($j=1, \dots, N$). The numerical values for the specific parameters were chosen randomly in certain ranges. The locations of the centers of the slabs, x_j , were in the range $-d/2 + jD < x_j < jD + d/2$, where D denotes the average distance between the centers of the j th and $(j+1)$ th scatterers. Exploring the scale invariance of the Maxwell equations, we will measure from now on all numerical values of the length in units of the distance D . The index variation was chosen in the range $1.3 < n_j < 1.5$ and the slab width w_j was in the range $0.1 < w_j/D < 0.3$. Each particular realization of the N layers is characterized by the set of $3N$ random numbers $\{x, w, n\}$. For simplicity, we neglect the homogeneous dispersion arising from a frequency-dependent index of refraction; however, due to the spatial dependence of the index of refraction, the total reflection depends very strongly on the frequency.

We assume that the incoming electromagnetic field travels perpendicular to the interfaces. This allows us to analyze the dynamics strictly in one dimension where the scattering angle is 0° or 180° , and we consider the electric field vector parallel to the slab-vacuum interface. Due to this symmetry, the problem can be investigated numerically using the transfer matrix approach by matching electric fields at the interfaces [18].

The reflection coefficient $R(\omega, \{x, w, n\})$ as a function of the laser frequency ω is shown in Fig. 1. It is an extremely oscillatory function of frequency and the reflection is characterized by many interferences, as is apparent from the

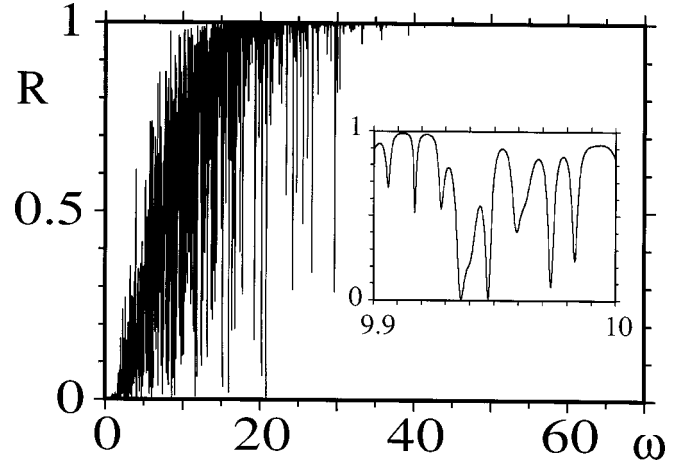


FIG. 1. The total reflection coefficient for a single medium consisting of $N=500$ dielectric layers with random width, index of refraction, and location as a function of the frequency. The frequency is displayed in units of c/D . The inset shows the small scale oscillations. (The random variables were uniformly distributed in the ranges $x_j = jD \pm d/2$, $n_j = 1.4 \pm 0.1$, $w_j = 0.01 \pm 0.005$, $d = D$.)

graph. Even though there is an overall tendency of the medium to become more reflective with increasing laser frequency, the large size of the fluctuations indicates the importance of the interferences between the individual scatterers for strictly monochromatic fields. The inset resolves these rapid oscillations on a very fine frequency range. It is quite remarkable that an increase of the frequency (in units of c/D) from $\omega=9.9212$ (with $R=0.9788$) by only $\Delta\omega/\omega = 0.3\%$ to $\omega=9.9476$ ($R=0.0055$) changes the medium from nearly opaque to nearly transparent.

In order to compare the Maxwell equations with the Boltzmann equation, it is advantageous to introduce the two auxiliary fields [19]

$$E(x, +, t) \equiv \frac{1}{2} \{ \sqrt{\varepsilon(x)} E_y(x, t) + B_z(x, t) / \sqrt{\mu} \}, \quad (2.3a)$$

$$E(x, -, t) \equiv \frac{1}{2} \{ \sqrt{\varepsilon(x)} E_y(x, t) - B_z(x, t) / \sqrt{\mu} \}. \quad (2.3b)$$

The wave equations (2.2a) and (2.2b) are equivalent to a set of coupled equations [20,21]

$$\begin{aligned} & \left(v(x) \frac{\partial}{\partial x} + \frac{\partial}{\partial t} \right) E(x, +, t) \\ &= -\frac{1}{2} \frac{dv(x)}{dx} \{ E(x, +, t) + E(x, -, t) \}, \end{aligned} \quad (2.4a)$$

$$\begin{aligned} & \left(v(x) \frac{\partial}{\partial x} - \frac{\partial}{\partial t} \right) E(x, -, t) \\ &= -\frac{1}{2} \frac{dv(x)}{dx} \{ E(x, +, t) + E(x, -, t) \}, \end{aligned} \quad (2.4b)$$

where $v(x) \equiv [\mu_0 \varepsilon(x)]^{-1/2}$ must be interpreted as the position-dependent velocity. The form of the generator in Eqs. (2.4) suggests that $E(x, +, t)$ and $E(x, -, t)$ represent fields propagating along the positive and negative x directions, respectively. $E^2(x, +, t)$ and $E^2(x, -, t)$ correspond to the right and left going photon fluxes, respectively. One can also show that $E^2(x, +, t) + E^2(x, -, t) = (1/2)[\varepsilon(x)E_y^2(x, t) + (1/\mu)B_z^2(x, t)]$ is the energy density and $v(x)[E^2(x, +, t) - E^2(x, -, t)] = (1/\mu)E_y(x, t)B_z(x, t)$ is the Poynting vector.

Let us now show that the Boltzmann equation can be brought into a similar form. In general, this equation models the collection of many individual scatterers only by its average properties. In the absence of absorption, only three parameters characterize a scattering medium: the propagation speed in between two scattering events c , the scattering coefficient μ_s (the inverse of the scattering length), and the scattering phase function $p(\mathbf{\Omega}, \mathbf{\Omega}')$. The last is the conditional probability that an incoming particle associated with direction $\mathbf{\Omega}$ is scattered into the direction $\mathbf{\Omega}'$. The three-dimensional Boltzmann equation (radiative transfer equation) [1] is given by

$$\left(\frac{1}{c} \frac{\partial}{\partial t} + \mathbf{\Omega} \cdot \nabla \right) I(\mathbf{r}, \mathbf{\Omega}, t) = \mu_s \int d\mathbf{\Omega}' p(\mathbf{\Omega}, \mathbf{\Omega}') I(\mathbf{r}, \mathbf{\Omega}', t) - \mu_s I(\mathbf{r}, \mathbf{\Omega}, t), \quad (2.5)$$

where $I(\mathbf{r}, \mathbf{\Omega}, t)$ represents the local radiation flux density propagating in the $\mathbf{\Omega}$ direction. The Boltzmann equation for a one-dimensional medium can be obtained by restricting the scattering phase function to permit only forward and backward scattering [22]:

$$p(\mathbf{\Omega}, \mathbf{\Omega}') = \frac{1}{4\pi} (1-g) \delta(\cos \vartheta + 1) + \frac{1}{4\pi} (1+g) \delta(\cos \vartheta - 1), \quad (2.6)$$

where $\cos \vartheta \equiv \mathbf{\Omega} \cdot \mathbf{\Omega}'$. The anisotropy factor g is defined as the average cosine of the scattering angle ϑ , $g \equiv \int d\mathbf{\Omega}' p(\mathbf{\Omega}, \mathbf{\Omega}') \cos \vartheta$. With this bidirectional phase function, the Boltzmann equation can be expressed as a simple coupled set of differential equations in space x and time t :

$$\left(\frac{1}{c} \frac{\partial}{\partial t} + \frac{\partial}{\partial x} \right) I(x, +, t) = -\mu I(x, +, t) + \mu I(x, -, t), \quad (2.7a)$$

$$\left(\frac{1}{c} \frac{\partial}{\partial t} - \frac{\partial}{\partial x} \right) I(x, -, t) = \mu I(x, +, t) - \mu I(x, -, t), \quad (2.7b)$$

where we have defined $\mu \equiv \mu_s(1-g)/2$ as the effective scattering coefficient and where $I(x, \pm, t)$ represents the photon flux along the positive and negative x directions. These two equations have an obvious interpretation: $I(x, +, t)$ couples to $I(x, -, t)$, and vice versa. By eliminating the diagonal

coupling one can derive a useful iterative scheme in which the n th order solution corresponds directly to the photon paths that have scattered n times [23]. In this formalism, the parameter μ is directly related to the reversal probability.

The reflection probability in the steady state ($\partial/\partial t = 0$), for a medium of length L , can be obtained from Eqs. (2.7) using the boundary conditions $I(x=0, +) = 1$ and $I(x=L, -) = 0$. The reflection coefficient $I(x=0, -) = \mu L / [1 + \mu L]$ is the main prediction of the Boltzmann theory [14], and we will discuss its implications in Sec. IV.

Let us now comment on the formal similarity between the set of two coupled equations according to the macroscopic and microscopic theories of Eqs. (2.4) and Eqs. (2.7), respectively. Both equations are linear and have nearly identical spatiotemporal generators (left hand sides), except that the velocity $v(x)$ is a true microscopic quantity rapidly changing on the smallest length scale. However, the coupling matrices on the right hand side are different. In the Maxwell equations, the coupling strength between the right and left going fields is given by the spatial gradient of the velocity $(1/2)dv(x)/dx$. We also note that the coupling matrix is real and symmetric with eigenvalues 0 and $-(1/2)dv(x)/dx$, whereas the corresponding 2×2 coupling matrix for the Boltzmann theory [Eqs. (2.7)] is nilpotent with the degenerate eigenvalues 0.

The different structures of the two propagators have consequences with respect to the nature of the iterative terms. In the Maxwell theory, the fields $E(x, +, t)$ and $E(x, -, t)$ can take positive and negative values, and therefore contributions associated with n th order scattering can destructively interfere with lower orders [19]. In the Boltzmann theory, the structure of the propagator preserves the sign of the two radiation flux densities $I(x, +, t)$ and $I(x, -, t)$, and therefore all n th order scattering contributions add up in an accumulative way.

III. FREQUENCY AND ENSEMBLE AVERAGE OF THE MAXWELL SOLUTION

Let us now discuss how two different averaging schemes can convert the oscillatory reflection coefficient displayed in Fig. 1 for a single medium into a smooth function, which then permits a direct comparison with the prediction of the Boltzmann equation. In addition to the erratic frequency dependence, the total reflection coefficient for specific realization of a single random medium is a function of a set of $3N$ random numbers $\{x, w, n\}$. In order to eliminate those aspects of the response that vary from specific realization to realization, we can construct a more universal reflection coefficient by averaging over all microscopic degrees of freedom according to their probability distribution function $\rho(\{x, w, n\})$:

$$\langle R(\omega) \rangle \equiv \left[\prod_j^N \int dx_j \int dw_j \int dn_j \right] \times \rho(\{x, w, n\}) R(\omega, \{x, w, n\}). \quad (3.1)$$

We have performed this ensemble average numerically by computing the average reflection coefficient from 5000 different random media, each characterized by 3×500 indepen-

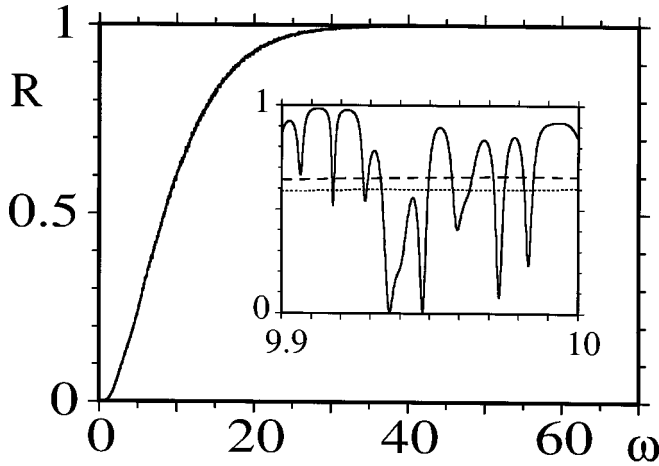


FIG. 2. The frequency and ensemble average of the total reflection coefficient for a medium of the type of Fig. 1. The frequency is displayed in units of c/D . The inset shows the two averaged graphs together with the small scale oscillations characteristic of a single medium. The dotted line in the graph represents the ensemble averaged reflection coefficient and the dashed line the frequency averaged result. (Same random parameters as in Fig. 1.)

dent random numbers. The result of this quite CPU consuming task is displayed in Fig. 2. Comparing with the graph in Fig. 1, we see that all the quasierratic oscillations characteristic of a single medium have been removed, and the graph suggests that it could even match the average behavior of the reflection coefficient with respect to the frequency.

So far the reflection was calculated for a strictly monochromatic input laser field. In order to compute the response of a quasimonochromatic field with a frequency width δ around the center frequency ω_c , we can average the reflection for a single random medium over a small frequency range if the phases of the complex reflection amplitudes vary sufficiently fast with frequency:

$$R(\omega_c, \delta, \{x, w, n\}) \equiv \int d\omega \rho(\omega, \omega_c, \delta) R(\omega, \{x, w, n\}). \quad (3.2)$$

Please note that this quantity is (at least formally) still a function of all $3N$ parameters $\{x, w, n\}$ and therefore it could vary from medium to medium. To keep our analysis as simple as possible, we have assumed that the frequencies are uniformly distributed, such that $\rho(\omega, \omega_c, \delta) = [\theta(\omega - \omega_c + \delta/2) - \theta(\omega - \omega_c - \delta/2)]/\delta$, where $\theta(\cdot)$ denotes the Heaviside unit step function. The frequency average $R(\omega_c, \delta, \{x, w, n\})$ was superimposed on the graph on Fig. 2. Two important observations are in order. First, the numerical data suggest that the frequency averaging removes the erratic oscillations characteristic of a single random medium. Second, it turns out that for the range of parameters discussed here, the two curves $R(\omega_c, \delta, \{x, w, n\})$ and $\langle R(\omega) \rangle$ are remarkably similar—if not identical—to each other.

This numerical observation opens the door to finding analytical solutions to the universal function $\langle R(\omega) \rangle$ and also provides the key for a comparison with the Boltzmann theory as we will discuss in Secs. IV and V. In other words, the

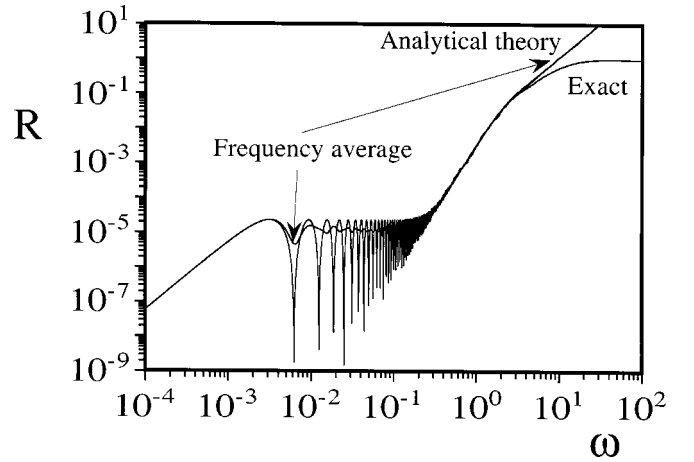


FIG. 3. The frequency and ensemble average of the total reflection coefficient for a simplified random medium based on the analytical solutions shown in the Eqs. (3.5) and (3.6). For comparison the exact reflection coefficient curve is also plotted. The frequency is shown in units of c/D . The scatterers were uniformly distributed in the ranges $x_j = j D \pm D/2$. All 500 scatterers have an index $n = 1.4$ and a width $w = 0.01D$.

complicated $3N$ averages can be replaced by an average over a single parameter, the frequency ω . This observation can become relevant for future analytical work on bridging the microscopic and macroscopic theories on the level of the corresponding equations of motion, as we will outline in Sec. V.

In order to obtain some analytical insight into this surprising similarity and to construct an approximate but analytical form of the “universal” reflection coefficient, we have constructed the first order iterative solution to the Maxwell equations. As we will show below, this solution is valid for those frequencies for which single scattering is sufficient to describe the overall reflected light. In other words, this is the regime in which typically the total reflection coefficient is less than 5%. The data in Fig. 3 suggest that we would expect the single scattering approximation to hold for frequencies in the range $0 < \omega < 2.3c/D$.

Solving the Maxwell equations (2.4) in the frequency regime ($\partial/\partial t = i\omega$) with the boundary conditions $E(x=0, +, \omega') = \delta(\omega - \omega')$ and $E(x=L, -, \omega') = 0$, we obtain the following amplitude for the reflected light which has experienced only a single scattering event:

$$\begin{aligned} E^{(1)}(x=0, -, \omega) &\equiv r^{(1)}(\omega) \\ &= \int_0^L dx v'(x)/v(x) \\ &\quad \times \exp\left[-i2\omega \int_0^x dx'/v(x')\right]. \end{aligned} \quad (3.3)$$

The integral in the exponent $\int_0^x dx'/v(x')$ is the time a pulse of velocity $v(x)$ takes to travel from $x=0$ to x without scattering, such that the exponent in Eq. (3.3) corresponds to the phase that the reflected light obtains after having traveled

from $x=0$ to x and back to $x=0$. The term $v'(x)/v(x)$ can be interpreted as a reversal probability at location x , as discussed above.

In order to obtain simple and illustrative analytical solutions without any loss of generality, let us assume that the width of each slab w_j is very small, such that the medium's index of refraction $n(x) = 1 + \sum_{j=1}^N (n_j - 1) [\theta(x - x_j + w_j/2) - \theta(x - x_j - w_j/2)]$ can be approximated by $n(x) = 1 + \sum_{j=1}^N (n_j - 1) w_{\text{eff},j} \delta(x - x_j)$. Let us also freeze the indices of refraction $n_j \equiv n$ and the widths $w_j \equiv w$, while leaving the center positions of the slabs randomly located at $x_j = jD + \xi$, where ξ is a uniformly distributed random number in the range $-d/2 < \xi < d/2$. These assumptions turn out to be not too restrictive, as the basic structure of the graphs in Figs. 1 and 2 is mainly due to the positions of the slabs and less due to the fluctuations in the width or the index of refraction.

The effective "width" w_{eff} can be related to the true thickness w of each slab if we equate the reflection coefficient for a single slab with the small but finite width w , given by $(n^2 - 1)^2 (\omega w/c)^2 / 4$, with the reflection coefficient for the δ -function scatterer, according to $|r^{(1)}(\omega)|^2 = (n - 1)^2 (w_{\text{eff}} \omega/c)^2$. We obtain the relation $w_{\text{eff}} = w(n + 1)/2$.

Using the above expression for $v(x) = c/n(x)$, the integral (3.3) can be calculated, and we obtain the simple form

$$r^{(1)}(\omega, \beta, \{x\}) = \omega^2 \beta^2 / c^2 \sum_{j=1}^N \exp[2i\omega(x_j + j\beta)/c], \quad (3.4)$$

where we have defined $\beta \equiv (n - 1)w_{\text{eff}} = w(n^2 - 1)/2$. This solution permits us now to calculate the ensemble average as well as the frequency average fully analytically.

The ensemble average defined in Eq. (3.1) can be obtained as

$$\begin{aligned} \langle R^{(1)}(\omega) \rangle &= \beta^2 \omega^2 / c^2 \{ N [1 - \sin^2(\omega d/c) / (\omega d/c)^2] \\ &\quad + \sin^2(\omega d/c) \sin^2(\omega(D + \beta)dN/c) / [\omega d/c \\ &\quad \times \sin(\omega(D + \beta)d/c)]^2 \}. \end{aligned} \quad (3.5)$$

This universal reflection coefficient reveals several interesting features. Four clearly distinct frequency regimes (in units of c/D) can be obtained from Fig. 3. In the small frequency limit ($\omega < 1.26 \times 10^{-3}$) the reflected intensity grows quadratically with the frequency; the next regime ($1.26 \times 10^{-3} < \omega < 0.251$) is characterized by oscillations with equal amplitude ($\approx 1.58 \times 10^{-5}$) and a frequency difference from peak to peak of 0.006. In the regime $0.251 < \omega < 3.98$, the intensity grows initially with the fourth power of the frequency; and for large frequencies ($3.98 > \omega$) the intensity again grows quadratically with the frequency.

The small and large frequency limits suggest a transition from a fully coherent to an incoherent response of the medium. In the small frequency limit [$\omega(\beta + D)N/c < 0.1$], we obtain that the total reflected intensity $\langle R^{(1)}(\omega) \rangle$ is given by the square of the sum of the individual electric field amplitudes associated with reversals at locations x_j , $\langle R^{(1)}(\omega) \rangle$

$= \omega^2 \beta^2 N^2 / c^2$. In this limit the wavelength $2\pi c/\omega$ is larger than the entire medium, and the total reflected intensity is identical for any random arrangement of N scatterers.

In the large frequency limit ($\omega d/c \gg 1$), we obtain that the total reflected intensity $\langle R^{(1)}(\omega) \rangle$ is given by the sum of the squared individual electric field amplitudes associated with reversals at locations x_j , $\langle R^{(1)}(\omega) \rangle = \omega^2 \beta^2 N / c^2$. In this limit the wavelength is small enough that the individual locations of the scatters can be resolved, but the phases vary so rapidly from scattering location to scattering location that the coherent contributions in $\omega^2 \beta^2 / c^2 \sum_{j=1}^N \sum_{j'=1}^N \exp[2i\omega[(x_j - x_{j'}) + (j - j')\beta/c]]$ average out to zero for $j \neq j'$ and only the diagonal terms ($j = j'$) contribute.

The two intermediate frequency regimes are more difficult to interpret. The oscillatory regime requiring $0.1 < N\omega d/c$ and $\omega d/c < 0.1$ is described by $\langle R^{(1)}(\omega) \rangle = \{\beta/(\beta + D) \sin[\omega(\beta + D)N/c]\}^2$. We should note that this oscillation frequency is identical for each individual medium. In other words, it is independent of the ensemble averaging procedure. For even larger frequencies ($0.1 < \omega d/c$) the dependence $\langle R^{(1)}(\omega) \rangle = \beta^2 \omega^2 N [\omega^2 - \sin^2(\omega d/c) / d^2] / c^2$ is accurate. The fourth power regime follows trivially from this expression, $\langle R^{(1)}(\omega) \rangle = (1/3) \beta^2 d^2 \omega^4 / c^4$.

As we have mentioned above, $\langle R^{(1)}(\omega) \rangle$ is a valid approximation only if higher order scattering contributions can be neglected, i.e., the reflection coefficient is small enough. In order to examine the frequency regime of validity of $\langle R^{(1)}(\omega) \rangle$, we have compared it in Fig. 3 to the exact total reflection intensity $\langle R(\omega) \rangle$ (containing all orders). The agreement with the analytical curve is valid in all frequency regimes up to $\omega = 2.3c/D$ and roughly corresponds to $\langle R(\omega) \rangle \leq 5\%$, as suggested above.

Let us now analyze the first order reflected intensity obtained from averaging over a range of frequencies. The resulting analytical expression is given by a double sum,

$$\begin{aligned} R^{(1)}(\omega_c, \delta, \{x\}) &\equiv \int d\omega \rho(\omega, \omega_c, \delta) |r^{(1)}(\omega, \beta, \{x\})|^2 \\ &= \omega^2 \beta^2 N / c^2 + \omega^2 \beta^2 / c^2 \\ &\quad \times \sum_{j=1}^N \sum_{j=1, j' \neq j}^N \exp[2i\omega_c[(x_j - x_{j'}) + (j - j')\beta/c]] \\ &\quad \times \sin\{\delta[(x_j - x_{j'}) + (j - j')\beta/c]\} / \{\delta[(x_j - x_{j'}) \\ &\quad + (j - j')\beta/c]\}. \end{aligned} \quad (3.6)$$

In Fig. 3 we have graphed this function for the frequency width $\delta = \omega_c/10$. The agreement with the analytical form of Eq. (3.5) is superb for all frequencies. We should mention that, even though the reflection coefficient $R^{(1)}(\omega_c, \delta, \{x\})$ does depend on the frequency width δ , for a very small width the fine oscillations characteristic of a single random medium are reconstructed, and for a very large width the overall important frequency dependence is averaged out. However,

we found that there is an intermediate regime, for which the results for all practical purposes do not depend on the width δ .

We should point out that the close relationship between the frequency and ensemble average of the reflection coefficient could be interpreted as a weak form of ergodicity. In statistical mechanics [24], a random process $z(t)$ is called stationary if the ensemble average of any function of the random variables $z(t_1), z(t_2), \dots, z(t_N)$ is invariant under a time translation. As a special case, the autocorrelation function depends only on the difference of the two arguments $t_2 - t_1$ for a stationary process. Consequently, the probability distribution for the random number z cannot depend on the variable t . A stationary random process is generally called ergodic, if the autocorrelation function decays to zero sufficiently rapidly with increasing time. Then all realizations of the random process look somewhat similar and differ only in detail, and a suitable time average $\lim_{T \rightarrow \infty} (1/T) \int_{-T/2}^{T/2} dt \dots$ is identical to the average over all possible realizations (ensemble average) $\langle \dots \rangle$.

How do these mathematical definitions apply to our dielectric medium? It is important to note that we have two different random processes involved. The first one is the fluctuating index of refraction $n(x)$, which is a function of the position x and varies randomly for different realizations of the medium. For the simplest case of an index $n(x)$ that jumps instantaneously between two fixed values (random telegraph signal), one can show [5] that for an infinitely long medium this process would be stationary as well as fully ergodic.

The second random process is the reflection coefficient as a function of the frequency. A particular realization was displayed in Fig. 1 for a finite length medium. Clearly, this process is not stationary as its ensemble average does depend on the frequency and the data show a preferred origin of the frequency ($\omega=0$). Even if we were to subtract out this average value, the process $R(\omega) - \langle R(\omega) \rangle$ still does not qualify to be called stationary, because the character of the fluctuations changes with the frequency, i.e., the amplitude of the fluctuations decreases with increasing frequency. Therefore our system is *not* ergodic in the traditional mathematical sense. If it were, the ensemble $\langle \dots \rangle$ and frequency $\lim_{\delta \rightarrow \infty} (1/\delta) \int_{-\delta/2}^{\delta/2} d\omega \dots$ averages should agree exactly with each other for any number of slabs N . One can see from Fig. 2 that this is not the case, as the numerical agreement is observed only for local frequency averages around ω_c .

IV. COMPARISON OF THE AVERAGED MAXWELL SOLUTION WITH THE BOLTZMANN EQUATION

As noted above, the prediction of the Boltzmann equation for the reflection coefficient is simply $\mu L / (1 + \mu L)$, where $L (=ND)$ denotes the total length of the medium, which is the number of slabs multiplied by the average distance D between them. If the Boltzmann equation is correct, then it must be possible to find an appropriate value for the scattering coefficient μ , such that the exact ensemble averaged reflection $\langle R(\omega) \rangle$ is identical to $\mu L / (1 + \mu L)$. In other words, for the Boltzmann theory to be completely accurate, the ef-

fective scattering coefficient must be

$$\mu(\omega, L) \equiv \langle R(\omega) \rangle / \{L[1 - \langle R(\omega) \rangle]\}. \quad (4.1)$$

Now it is crucial to notice that the scattering coefficient should depend only on averages over truly microscopic quantities, such as the density of scatterers and their average index of refraction or width. In principle, of course, it is always possible to construct an effective μ according to Eq. (4.1). However, in order for the Boltzmann equation to be valid, the scattering parameter should *not* depend on the length of the medium L and should be derived by a suitable averaging over a microscopic region in space only. In other words, the derivative $|\partial \mu(\omega, L) / \partial L|$ could be defined as a quantitative measure for the degree of validity of the Boltzmann equation. We have graphed the ratio of this derivative and $\mu(\omega, L)$ as a function of the frequency but did not find the data very useful to characterize the regime in which the Boltzmann equation could be valid.

Instead of using the total reflection coefficient for the medium, let us now derive the scattering coefficient from a truly microscopic analysis. In one dimension the total scattering cross section can be defined as $\sigma_{\text{tot}} \equiv |f(+)|^2 + |f(-)|^2$, where $f(+)$ and $f(-)$ are the forward and backward scattering amplitudes, respectively. This relationship follows from a partial wave decomposition and satisfies the corresponding optical theorem [25]. The anisotropy factor can be obtained as $g = \{\cos(0)|f(+)|^2 + \cos(\pi)|f(-)|^2\} / \sigma_{\text{tot}}$, and using these two relations it is easily seen that $\sigma_{\text{tot}}(1-g)/2 = |f(-)|^2$. In the literature on the Boltzmann theory [8], it is often suggested that the scattering coefficient μ_s should be related to the product of the density of the scatterers ρ and the average total cross section $\langle \sigma_{\text{tot}} \rangle$ of all the individual scatterers, $\mu_s = \rho \langle \sigma_{\text{tot}} \rangle$. We will test this hypothesis below and show how a modified scattering coefficient can improve the agreement with the exact data obtained from the Maxwell theory.

For identical scatterers, the reduced scattering coefficient $\mu = \mu_s(1-g)/2$ is directly related to the reflection coefficient of a single slab via $\mu = \rho R(\omega)$, where the density ρ denotes the number of scatterers per unit length. This follows immediately by relating the complex frequency-dependent reflection and transmission amplitudes to the scattering amplitudes via $f(+)=t(\omega)-1$ and $f(-)=r(\omega)$. Thus a direct relationship is established between the macroscopic scattering coefficient and the microscopic variables such as the index of refraction and size of the scatterer.

In Fig. 4 we have graphed the exact Maxwell ensemble averaged reflection coefficient for a medium of $N=1000$ dielectric layers together with the prediction of the usual Boltzmann equation,

$$R_B(\omega) = \rho R_1(\omega) L / [1 + \rho R_1(\omega) L], \quad (4.2)$$

where the medium's length $L=ND$ and we have used the exact reflection coefficient of a single slab denoted by $R_1(\omega)$:

$$R_1(\omega) = \frac{\left[\frac{(1-n)/(1+n)\{1 - \exp[(2i\omega/c)nw]\}}{1 - [(1-n)^2/(1+n)^2] \exp[(2i\omega/c)nw]} \right]^2}{\left[\frac{(1-n)/(1+n)\{1 - \exp[(2i\omega/c)nw]\}}{1 - [(1-n)^2/(1+n)^2] \exp[(2i\omega/c)nw]} \right]^2}. \quad (4.3)$$

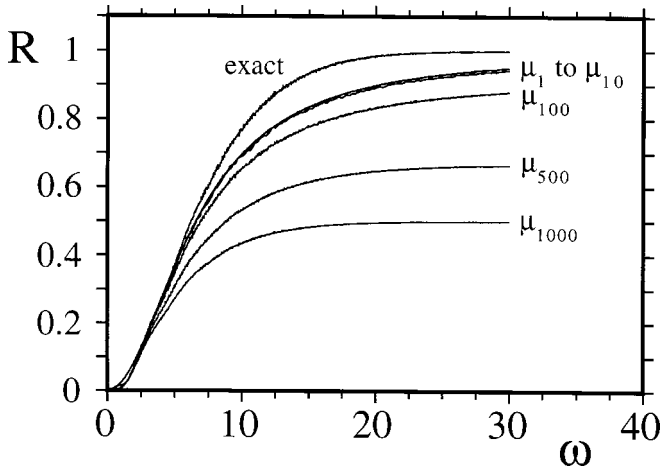


FIG. 4. Comparison of the predictions of the Boltzmann equation with the exact reflection coefficient. The various graphs according to the Boltzmann equation differ by the size of the microscopic cell that has been taken into account to compute the scattering coefficient μ . The subscripts indicate the number of slabs over which the microscopic reflection coefficient was computed. (The parameters are as in Fig. 3 except for the number of scatterers $N=1000$.)

The agreement between the exact curve and the usual Boltzmann prediction is good only for a certain frequency range.

Note that according to the usual Boltzmann theory the scattering coefficient is supposed to be computed from the average cross section of a *single* scatterer, $\mu_1 = \rho_1 R_1$. In other words, potentially important length scales such as the average spacing D between two or more neighboring scatterers are not included. If the computation of the cross section is not artificially restricted to a single scatterer but it is actually computed from a slightly larger microscopic cell that contains several scatterers, then the resulting scattering coefficient can improve the validity of the Boltzmann equation significantly for small frequencies.

This is shown by Fig. 5, for which the scattering coefficient has been calculated numerically from the total reflection coefficient for $n=2, 5$, and 10 scatterers, denoted by μ_2, μ_5 , and μ_{10} , and with effective densities $\rho_2 = (N/2)/L$, $\rho_5 = (N/5)/L$, and $\rho_{10} = (N/10)/L$. The improved scattering coefficients μ_m now contain the important information about the average interslab spacing D . As a result, the agreement with the exact data extends to much smaller frequencies.

One could incorrectly conjecture that the Boltzmann prediction can be continuously improved if one only increases the number of slabs in the calculation of the effective scattering coefficient. The failure of the Boltzmann theory is not associated with a “nonperfect” computation of μ_s , but with the fact that the total reflection coefficient according to the Boltzmann equation must take the specific functional form given by Eq. (4.2), which requires a very peculiar dependence on the medium’s length L . If we exaggerate the size of the microscopic cell to include all N slabs leading to R_N , and $\rho_N = 1/L$, correspondingly, we obtain $R_B = R_N/(1+R_N)$, which is inconsistent with the requirement $R_B = R_N$. In fact,

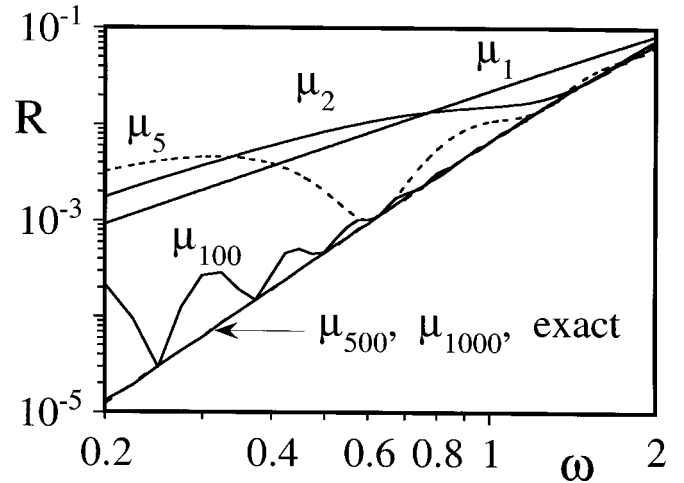


FIG. 5. Same data as in Fig. 4 but for a smaller frequency range. For small frequencies the Boltzmann theory becomes more suitable for increasing size of the microscopic cell used for the calculation of the effective scattering coefficient.

the Boltzmann theory can be improved for small frequencies as we showed, but it still has its principal limits for larger frequencies. Independently, we have suggested numerically that the agreement between Boltzmann and Maxwell theories can also be improved if the ratio of the slabs’ width to their spacing is reduced [14].

V. SUMMARY AND OUTLOOK

We should finish this report with an outlook on future work. We note that the medium discussed in this work cannot convert a strictly monochromatic input field to incoherent light, in the sense that no new frequencies can be generated in a linear medium. A strictly monochromatic input field always leaves the medium as fully monochromatic, even though with a reduced amplitude. The random medium can act only as a linear frequency filter, in the sense that the reflected intensity at certain frequency components can be reduced in the transmitted or reflected light beams. In other words, the infinite coherence length characteristic of a monochromatic input field cannot be reduced to a finite value. As a consequence, the Boltzmann equation cannot be expected to model correctly the response of a monochromatic field for a single medium, for which we have shown that the reflection coefficient exhibits extreme oscillatory variations as a function of the frequency.

However, if the input field is only quasimonochromatic with a finite width δ , the frequency averaged reflection coefficient will describe the total reflected intensity appropriately, which then—at least in principle—can also be modeled by the Boltzmann equation. We note, however, that the difference between the smallest and the largest frequency components of an input field obviously cannot be increased by the medium.

Let us now return to our long term goal of “deriving” the Boltzmann equation from the Maxwell equations as mentioned in the Introduction. One of the basic results of this work is that the data for the complicated ensemble average of the

this reflection coefficient including all microscopic degrees of freedom can be computed much more efficiently by an average over a single parameter, the laser frequency ω . Using this knowledge, the first steps toward the goal could be to rewrite the linear Maxwell equations (2.4) in terms of the right and left going photon fluxes $E^2(x, +, t)$ and $E^2(x, -, t)$, respectively. The resulting nonlinear equations are still microscopic, as they contain the random function $v(x)$. The strategy would be to “appropriately” average these equations over a frequency range; then in a certain limit an equation for the averaged fluxes might resemble the Boltzmann equation. Our numerical work certainly suggests that parameter choices exist for which such an agreement could be found. This derivation would also provide a computational approach to computing the optimum scattering coefficient from microscopic properties as well as correction terms that increase the range of validity of the Boltzmann equation.

Another important question concerns the applicability of

the approach to higher dimensional systems. At the moment we do not see how our approach can be directly generalized to systems of higher dimensions without simplifying symmetries. The key challenge to deriving the Boltzmann equation from microscopic principles, however, already manifests itself in one spatial dimension, and we see no reason presently to unnecessarily complicate our future analysis by introducing more spatial dimensions. All these challenges will be the subject of future investigations.

ACKNOWLEDGMENTS

We acknowledge helpful conversations with H. Matsuoka. This work has been supported by the NSF under Grant No. PHY-0139596, the DOE under Grant No. DE-FG03-98SF21519, and BLV. We also acknowledge support from the Research Corporation for Cottrell Science Awards and ISU for URG's.

-
- [1] A. Ishimaru, *Wave Propagation and Scattering in Random Media*, Vols. 1 and 2 (Academic, New York, 1978).
 - [2] P. Sheng *et al.*, in *Scattering and Localization of Classical Waves in Random Media*, edited by P. Sheng (World Scientific, Singapore, 1990).
 - [3] P. Yeh, *Optical Waves in Layered Media* (Wiley, New York, 1988).
 - [4] For a review, see, e.g., M. C. van Rossum and T. M. Nieuwenhuizen, *Rev. Mod. Phys.* **71**, 313 (1999).
 - [5] L. Mandel and E. Wolf, *Optical Coherence and Quantum Optics* (Cambridge University Press, Cambridge, England, 1995), Chap. 5.
 - [6] S. Chandrasekhar, *Radiative Transfer* (Clarendon Press, Oxford, 1950).
 - [7] See P. M. Morse and H. Feshbach, *Methods of Theoretical Physics* (McGraw-Hill, New York, 1953), Chaps. 2 and 12.
 - [8] For a review, see B. B. Das, F. Liu, and R. R. Alfano, *Rep. Prog. Phys.* **60**, 227 (1997).
 - [9] B. J. Tromberg, L. O. Svaasand, T. T. Tsay, and R. C. Haskell, *Appl. Opt.* **32**, 607 (1993).
 - [10] E. Gratton, W. Mantulin, M. J. van de Ven, J. Fishkin, M. Maris, and B. Chance, in *Proceedings of the Third International Conference on Peace through Mind/Brain Science*, edited by Hamamatsu Photonics (Hamamatsu, Hamamatsu City, Japan, 1990), p. 183; J. B. Fishkin, Ph.D. thesis, University of Illinois, 1994.
 - [11] A. Yodh and B. Chance, *Phys. Today* **48(3)**, 34 (1995).
 - [12] M. A. O'Leary, D. A. Boas, B. Chance, and A. G. Yodh, *Phys. Rev. Lett.* **69**, 2658 (1992); *Phys. Rev. E* **47**, R2999 (1993).
 - [13] E. Wolf, *Phys. Rev. D* **13**, 869 (1979).
 - [14] S. Menon, Q. Su, and R. Grobe, *Phys. Rev. E* **65**, 051917 (2002).
 - [15] S. Menon, S. M. Mandel, Q. Su, and R. Grobe, *Opt. Commun.* **205**, 25 (2002).
 - [16] For a numerical treatment of turbid media in higher dimensions, see W. Harshawardhan, Q. Su, and R. Grobe, *Phys. Rev. E* **62**, 8705 (2000).
 - [17] For an extensive reference list on the subject, see the web site www.fdfd.org
 - [18] See, for example, D. J. Griffiths, *Introduction to Electrodynamics* (Prentice-Hall, Upper Saddle River, NJ, 1999), Chap. 9.
 - [19] S. Menon, Q. Su, and R. Grobe (unpublished).
 - [20] S. He, S. Strom, and V. H. Weston, *Time Domain Wave Splitting and Inverse Problems* (Oxford University Press, Oxford, 1998); see also M. Gustafsson, Ph.D. thesis, Lund University, Sweden, 2000, available at http://www.tde.lth.se/home/mats/mypublications/Gustafsson_thesis.pdf
 - [21] R. Bellman and G. N. Wing, *An Introduction to Invariant Imbedding* (Wiley, New York, 1975).
 - [22] Q. Su, G. H. Rutherford, W. Harshawardhan, and R. Grobe, *Laser Phys.* **11**, 98 (2001).
 - [23] G. H. Rutherford, M. Marsalli, Q. Su, and R. Grobe, *Laser Phys.* **13**, 126 (2003).
 - [24] A. A. Sveshnikov, *Applied Methods of the Theory of Random Functions* (Pergamon, Oxford, 1966).
 - [25] J. H. Eberly, *Am. J. Phys.* **33**, 771 (1965).